ECS Transactions

(Invited) Towards the Physical Reliability of 3D-Integrated Systems: Broadband Dielectric Spectroscopic (BDS) Studies of Material Evolution and Reliability in Integrated Systems

To cite this article: Papa K. Amoah *et al* 2022 *ECS Trans.* **109** 41

ECS Transactions, 109 (2) 41-49 (2022)
10.1149/10902.0041ecst ©The Electrochemical Society

(Invited) Towards the Physical Reliability of 3D-Integrated Systems: Broadband Dielectric Spectroscopic (BDS) Studies of Material Evolution and Reliability in Integrated Systems

Papa K. Amoah,[1] Christopher Sunday,[2] Chukwudi A. Okoro,[2] Jungjoon Ahn,[2] Lin You,[2] Dmitry Veksler,[2] Joseph Kopanski,[2] and Yaw S. Obeng[2,z]

[1]Department of Electrical and Computer Engineering, Old Dominion University, Norfolk, VA 23529, USA

[2]Advanced Electronics Group, Physical Measurement Laboratory, National Institute for Standards and Technology, Gaithersburg, MD 20899, USA

[z]E-mail: yaw.obeng@nist.gov

Abstract

In this paper, we present an overview of our current research focus in developing non-destructive metrology for monitoring reliability issues in 3D- integrated electronic systems. We introduce a suite of non-destructive metrologies that can serve as early warning monitors for reliability issues. These Broadband Dielectric Spectroscopic (BDS) techniques are based on the application of high frequency microwaves (up to 40 GHz) to devices under various external stress, to probe impedance changes due to material and structural changes in integrated circuits. We illustrate the capabilities of the techniques with four case studies of potential reliability issues in 3D-IC interconnects.

Introduction

The improved performance and functionality of today's computers are attributed to materials and design innovation that have resulted in the increased density of transistors on chips. These technological innovations have shifted integrated circuits (ICs) from two-dimensional planar architecture to three dimensional (3D) by stacking of chips [1, 2]. As the device dimension continues to shrink and the chip area continues to decrease, the reliability of electronic circuitry has also shifted from being transistor-dominated to interconnect-dominated, constrained by challenges such as resistivity changes, unexplained early failures, unstable dielectric constants, stress-related failures, and thermal management issues. Thus, better insights into the properties of constituent materials under external stress, e.g., thermal stability of low-k materials, are needed to enable efficient device designs that proactively address performance and reliability gaps, as well as accommodate application extensions. Illustratively, there is a need for deeper understanding of how material properties and integration schemes contribute to the incidence of electromigration in interconnects and solder joints failures as we move away from copper as interconnect material, as well as into advanced packaging[3, 4]. Traditional reliability studies assume that the devices are constructed with faultless stable materials with uniform physiochemical properties, and the same extrinsic defects are most probably also responsible for limiting both die and packaged die yields[5 6]. These assumptions may no longer be valid, but we need appropriate non-destructive metrologies to further investigate them. Currently, there are no robust non-destructive, real-time in-line, metrology for accessing and quantifying these challenges[7]. Therefore, there is a need for effective metrology reliability analyses of the materials to determine the dominant failure mechanisms, and to predict appropriate device lifetimes [8].

Fortunately, the materials used in integrated circuit fabrication have unique electrical characteristics that are dependent on their dielectric properties, and microwave interrogation provides an opportunity to probe and to measure these properties. The material-microwave interactions of interest are based on changes in the electric dipole moment of the material in response to changes in an external field (i.e., permittivity). The applied electric field of the microwave, E, causes the dipolar moment, m, of the molecule to experience a torque, G, to orientate the dipolar moment parallel to the electric field. This instigates microwave absorption / energy dissipation during the rotation and orientation of the dipoles [9]. The dipole oscillates to keep up with the changing external magnetic fields, and at some critical frequency, the polarizability cannot be maintained, resulting in dielectric loss. These polarizable structures absorb microwaves to reorient and / or to rotate. At high frequencies, dielectric polarizability sets the scale for radiation absorption, while at low frequencies, it determines the nonlinear effect. Screening bound- and mobile charges set the scale for insulator-metal transitions, and mediate interactions among charge carriers and between charge carriers and phonons[10 11]. Broadband dielectric spectroscopy (BDS) provides both electrical and chemical information to guide the reliable integration of material into more robust designs for the intended applications, and for monitoring the manufacturing process. The microwave-dielectric material interactions are reasonably granular and uniquely suitable for studying the buried structures and material interfaces inherent in integrated circuit devices. For example, such interactions can detect the weak adhesion bonding; a steep gradient of S-parameters at low frequencies indicates a charge concentration around the imperfect region [12] . Thus, in principle, detailed studies of broadband RF interaction with integrated circuit devices under stress should enable fast in-situ detection of physico-chemical changes in the entire device such as defects, failure modes and mechanisms without the need for physical failure mode analysis (FMA).

Phenomenologically, we define a complex dielectric function that measures the electric displacement field due to the presence of an electric field in a dielectric material as written as Equation 1:

$$\varepsilon(\omega) = \varepsilon_1(\omega) + i\varepsilon_2(\omega) \quad (1)$$

where, $\omega = 2c\pi/\lambda$ is the frequency, c is the speed of light and λ is the wavelength, $\varepsilon_1(\omega)$ describes how much the material is polarized when an electric field is applied, and $\varepsilon_2(\omega)$ is related to the absorption of the material [13, 14]. The signal scattering from the electrical interfaces is summarized as a matrix of S-parameters that quantifies how RF energy propagates through a multiport network such as a vector network analyzer (VNA), e.g., insertion loss (S_{21}) or return loss (S_{11}). The S-parameters are readily transformed into electrical data[15] which can be further to provide mechanistically relevant metrics. For example, high frequency RF impedance measurements are more sensitive to physical degradation than low frequency (e.g., DC-resistance) measurements; a small incipient physical crack in a solder joint results in a readily detectable change in RF impedance, but not large enough to result in a DC-resistance open circuit and will not be detected by DCresistance[16, 17].

In the following, we illustrate how we have used BDS concepts to study various reliability[2] related issues in prototypical through silicon via (TSV) enabled 3D interconnects. Specifically, we study the accelerated aging of some of the materials used in the TSV fabrication. We also touch on using microwaves to detect buried broken interconnect lines, in situ, without the traditional sample preparation. In these studies, broadband microwaves (10 MHz to 40 GHz) were used.

Case Study 1: Demonstration of BDS in Mechanical Defects Detection in 3D Integrated System [18]

In this study, purposefully built two-level test structures, comprised of stacked dies connected through TSV, were subjected to thermal cycling in laboratory ambient conditions. RF measurements were performed every 500 thermal cycles, for up to a maximum of 2000 thermal cycles. All measurements were performed at room temperature.

Figure 1 shows the change in the magnitude of the insertion loss (S_{21}) as a function of thermal cycling and frequency for a typical die. In the main, the insertion loss (S_{21}) increases with the increasing number of thermal cycles; the S21 worsened at frequencies >20 GHz after 1000 thermal cycles. This RF signal transmission degradation with increasing thermal cycling is attributed to the increase in mechanical defects in the TSV daisy chain structure due to hydrostatic stress build-up in the TSV daisy chains with thermal exposure [19].

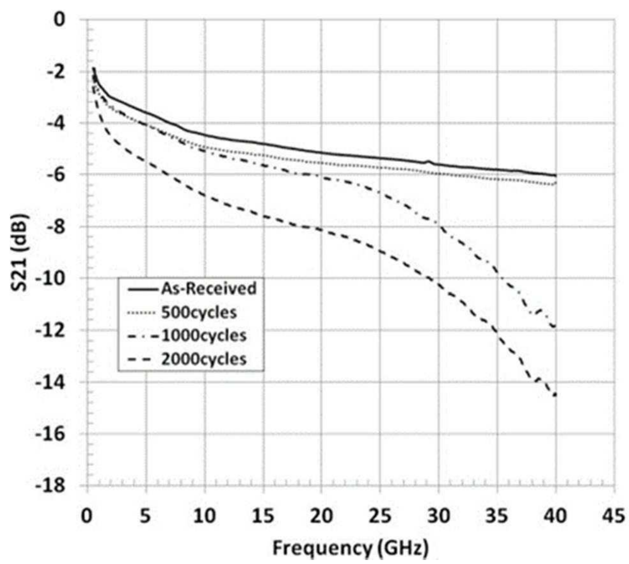

Figure: 1. Effect of thermal cycling on the magnitude of RF signal transmission coefficient (S_{21}) in a typical two-level stacked die.

Case Study 2: Characterization of Chemical Defects Detection in 3D Integrated System [20]

Isolating dielectrics such as low-temperature deposited silicon oxide films (SiO_x) are “difficult” materials from reliability perspectives due to the presence of numerous electrically active defects, dangling bonds and reactive functional groups[21]. Also, mechanical properties of encapsulation dielectric films affect device performance; for example, silicon oxide films with high local silanol content tend to be fragile and afford low packaging yields [22]. On exposure to microwaves, the macroscopic and local fields in the material are modified by relaxation events such as surface charge depolarization fields which oppose the applied field and result in net energy absorption (i.e., insertion losses) which can be leveraged to probe the nature of the dominant processes involved in the polarization-depolarization dynamics of dielectric materials [23].

In this study, BDS was applied in characterizing electrically active defects in the isolation dielectric that separates the co-axial copper fill in a through silicon via (TSV) from the host silicon in fully integrated 3D devices. The samples were thermally cycled and tested as described in Case Study 1 above. The S_{21} at the low frequency end (< 300 MHz) of the broadband RF spectrum were used as metrics to detect, characterize, and monitor the thermal evolution of defects in the liner dielectric. The observed change in the insertion loss (S21) spectra after 500 thermal cycles, in Figure 2, is most probably due to condensation reactions involving silanol functional groups in the amorphous as- deposited silicon oxide layer. Such amorphous silica (such as O_3/TEOS) are composed of a mixture of bulk tetrahedral SiO_4 units, and reactive metastable intermediates such as silanol (R_3Si–OH), siloxane bridge (R_3Si–O–SiR_3), and other hydrated surface functionalities. These intermediates react chemically when exposed to heat to result in totally different dielectric materials. Indeed, the some of the early high failures in prototypical devices could be due to such heat induced removal of silanols and non- bridging siloxane "defects" in the dielectric[24 25].

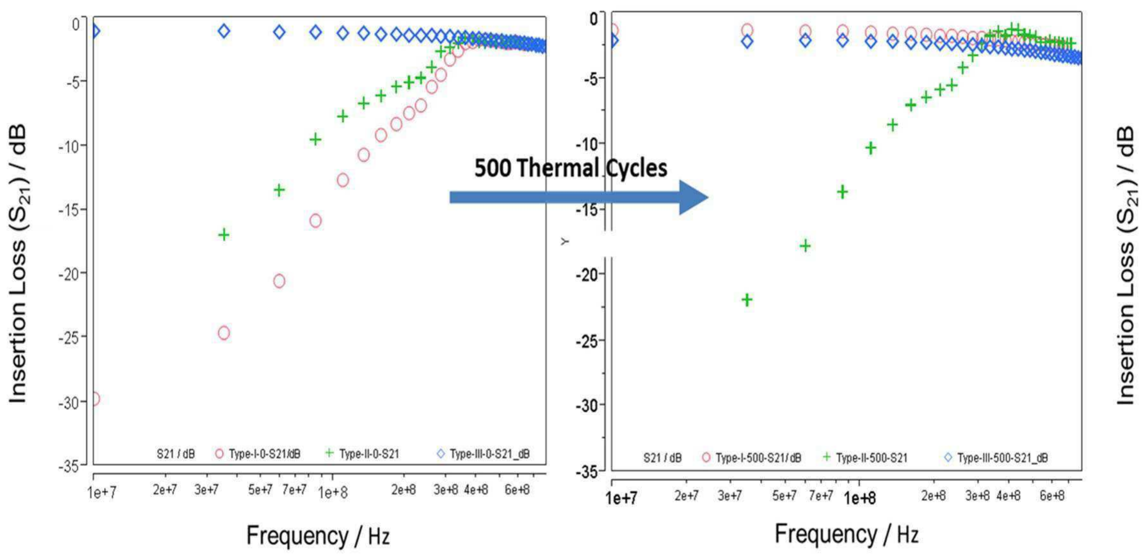

Figure 2: Comparison of the insertion loss (S_{21}) spectra of 'as-received' devices to devices after 500 thermal cycles showing changes in electrically active defect types and populations. Defect type- I is silanol (-Si-OH), type-II is silicon-carbide (-Si-R) and type-III is a siloxane (-Si-O-Si-). The S_{21} data suggests that type-I defect are precursors to the type-III, and the latter species react further to incorporate the siloxanes into tetrahedral silica centres.

Case Study 3: Thermal Stability of Prototypical Low-k Materials [26]

BDS was used to characterize the thermal stability of prototypical low-k dielectric films, as a function of material type and deposition methods, and to relate them to thermally-induced changes that occur in such films. By taking advantage of the changes in the microwave insertion losses, we examined the relationships between chemical and electrical properties from the impact of thermal annealing on the dielectric films [27]. For example, a sample comprised of hybrid porous carbon-doped inorganic oxides (SiOCH, with Si-C bonds, k< 4). Samples was stored and monitored at 200 °C. For this type of materials, the pendant group is thermally unstable, and it can degrade to generate porosity in the film which can be used to tune the dielectric constant to as low as 2.83 [28]. However, in air, competing aerobic peroxidation of the alkyl chains results in fragmentation without necessarily increasing film porosity. Such side reactions complicate any mechanistic studies, so in our experiments a nitrogen ambient was used to minimize aerobic oxidation of the sample.

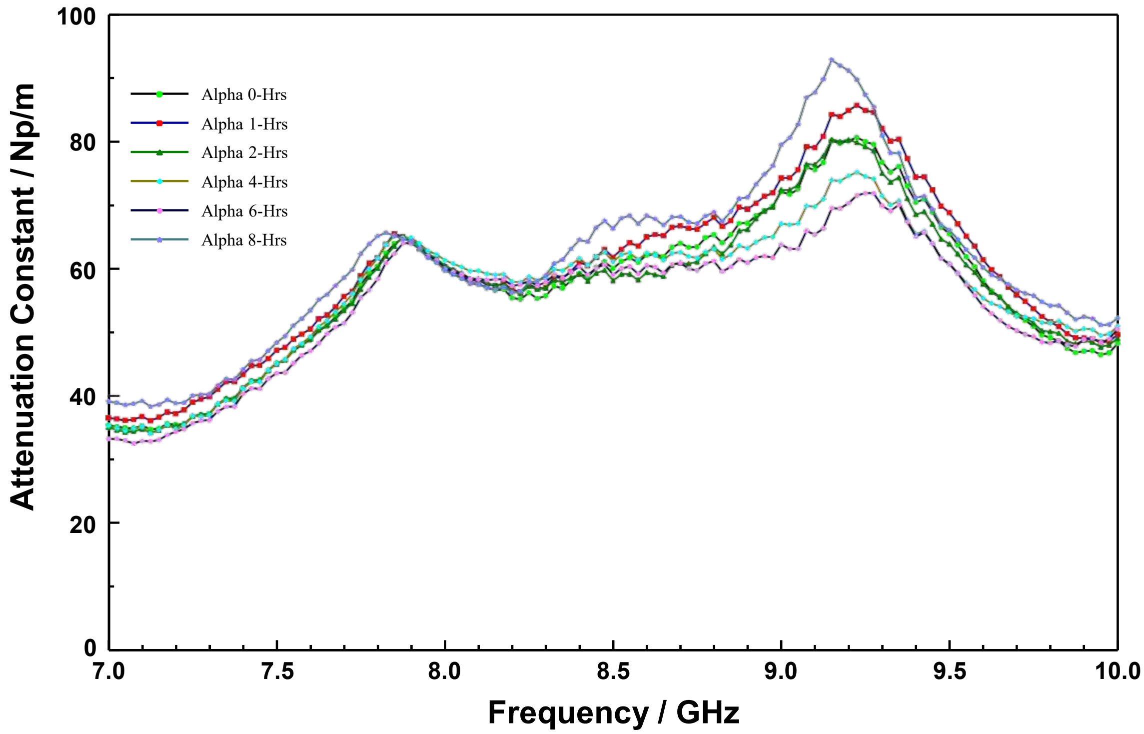

Figure 3: Microwave attenuation constant spectra of "as deposited" a prototypical (SOD) POSS thin film as a function of storage time s at 200 ºC in dry nitrogen.

As shown in Figure 3, the attenuation spectra of the "as deposited" spin on dielectric (SOD) film show resonance peaks around 7.8 and 9.2 GHz, respectively. While the resonance peak locations did not change much, the peak intensities varied over time with storage for the first 6 hours, but the resonance peaks shift to lower frequencies with a new peak around 8.5 GHz at the 8-hours storage mark. This suggests that the film started to decompose at around 8-hours of storage at 200 °C. This observation has implications for precursor material storage, IC manufacturing and packaging.

Case Study 4: Use of BDS in Subsurface Imaging of Metal Lines Embedded in Dielectric with the Scanning Microwave Microscope (SMM) [29]

Scanning microwave microscope (SMM) couples BDS to an AFM platform to generate spatially resolved images from the reflected microwave (S_{11}) signal amplitude and phase [30, 31]. In this work, a SMM operated at frequencies around 7.3 GHz was used to map the amplitude and phase the return loss (S_{11}) over a multi-level interconnect structure [32]. At these frequencies, the electromagnetic wave from the tip can propagate deep into the sample (predominantly dielectric) and interact with buried structures with a portion of the signal transmitted and reflected at each interface.

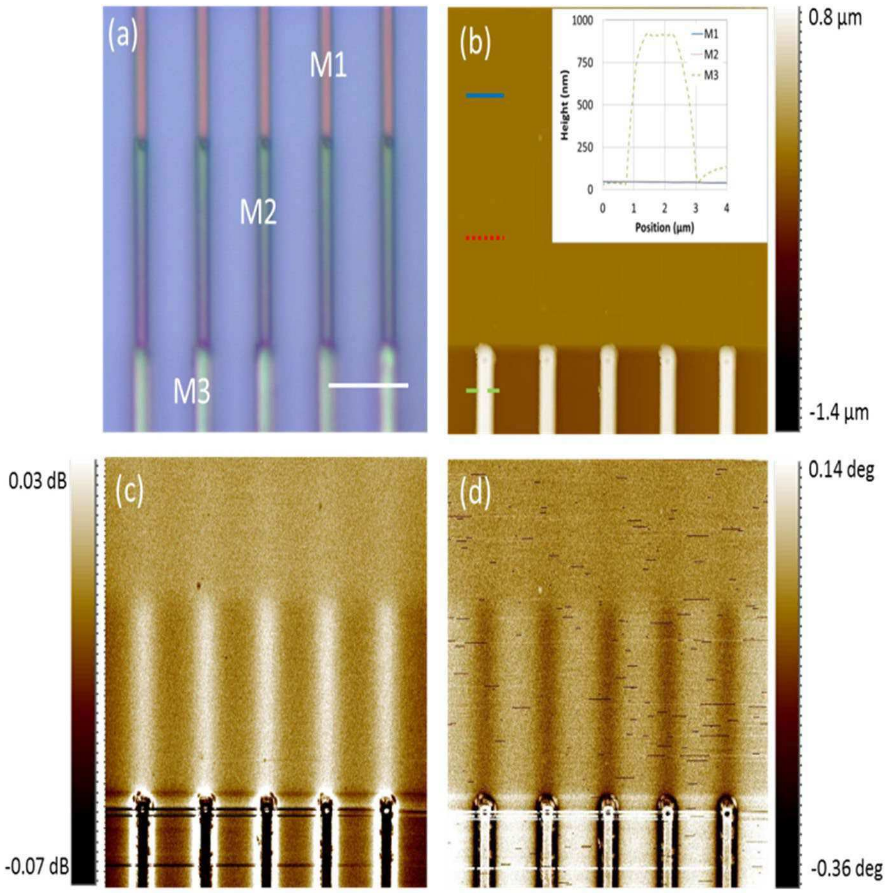

Figure 4: (a) Optical image of 'as-received' 4-level BEOL test structure: M3 is on the surface, while M2 and M1 lines are buried in oxide (M4 is not shown). The white scale bar is equal to 10 µm. (b) AFM topography shows the middle lines are totally buried by the planarized TEOS without any surface topography. The inset displays topographic line profiles at the site indicated with red, blue, and green lines, showing that the M3 is 900 nm above the dielectric surface while M2 and M1 has no topography. (c) Reflected S_{11} signal amplitude of the exposed M3 metal line and the buried M2 and M1 metal lines. (d) Reflected S_{11} phase of the exposed M3 metal line and the two buried metal lines. First order flattening has been applied to images (b), (c), and (d).

Figure 4 compares the optical, AFM topography, reflected microwave amplitude, and reflected microwave phase of the multi-level subsurface features on the "as received" test structure. The flatness of the device surface assures us that there will be no topography related artifacts in the microwave scans in the same area. The data shows a strong amplitude and phase contrast of the exposed metal line (M3), while the comparatively shallower metal lines (M2) show modest contrast. Of special interest is the faint contrast, and poorly resolved lines, located in the region of M1. This illustrates the potential of the near-field SMM at 7.3 GHz to probe buried metals lines at depths of about 2300 nm underneath PECVD TEOS dielectric. The spatial resolution in this work is substantially better than the literature value of better than 50 µm. The experimental results compared favorably to simulation results from a simple transmission line, lumped element model of the SMM. While this the methodology is interesting, the technique may not be suitable for inline use: it is slow and requires a specific test structure configuration.

Summary and Prognosis

The observations from this work extend the application scope of non-destructive broadband microwave-based metrology platform for understanding and quantification of aging of the constituent materials of prototypical IC devices. This could help, by modifying the process/integration or changing materials/designs, to avoid/delay the degradation at use conditions associated with the back-end-of-the-line (BEOL) metallization and advanced packaging. This is a promising platform that would allow us to gain insights into the thermal stability and reliability of emerging materials such as low- and ultra -low dielectric constant materials. With further development we should be able to quantify defects from the S-parameters. While the static BDS-based techniques can be used "in-situ" during accelerated aging while the device is still under stress, the scanning probe approach is too slow for in-line application.

Conflict of Interest Statement

Certain commercial equipment, instruments, or materials are identified in this report to specify the experimental procedure adequately. Such identification is not intended to imply recommendation or endorsement by the National Institute of Standards and Technology, nor is it intended to imply that the materials or equipment identified are necessarily the best available for the purpose.

References

1. Kumbhare, V. R.; Kumar, R.; Majumder, M. K.; Kumar, S.; Paltani, P. P.; Kaushik, B. K.; Sharma, R., High-Speed Interconnects: History, Evolution, and the Road Ahead. *IEEE Microwave Magazine* **2022,** *23* (8), 66-82.
2. Moreau, S.; Jourdon, J.; Lhostis, S.; Bouchu, D.; Ayoub, B.; Arnaud, L.; Frémont, H., Review—Hybrid Bonding-Based Interconnects: A Status on the Last Robustness and Reliability Achievements. *ECS Journal of Solid State Science and Technology* **2022,** *11* (2), 024001.
3. Tan, C. M.; Roy, A., Electromigration in ULSI interconnects. *Materials Science and Engineering: R: Reports* **2007,** *58* (1), 1-75.
4. Liu, Y.; Liang, L.; Irving, S.; Luk, T., 3D Modeling of electromigration combined with thermal–mechanical effect for IC device and package. *Microelectronics Reliability* **2008,** *48* (6), 811-824.
5. Huang, W.; Askin, R. G., Reliability analysis of electronic devices with multiple competing failure modes involving performance aging degradation. *Quality and Reliability Engineering International* **2003,** *19* (3), 241-254.
6. Wheeler, D.; Moffat, T. P.; Josell, D., Spatial-Temporal Modeling of Extreme Bottom-up Filling of Through-Silicon-Vias. *Journal of The Electrochemical Society* **2013,** *160* (12), 3260-3265.
7. Orji, N. G.; Badaroglu, M.; Barnes, B. M.; Beitia, C.; Bunday, B. D.; Celano, U.; Kline, R. J.; Neisser, M.; Obeng, Y.; Vladar, A. E., Metrology for the next generation of semiconductor devices. *Nature Electronics* **2018,** *1* (10), 532-547. 8. Shrestha, S. M.; Mallineni, J. K.; Yedidi, K. R.; Knisely, B.; Tatapudi, S.; Kuitche, J.; TamizhMani, G., Determination of Dominant Failure Modes Using FMECA on the Field Deployed c-Si Modules Under Hot-Dry Desert Climate. *IEEE Journal of Photovoltaics* **2015,** *5* (1), 174 - 182.
9. Marghany, M., Chapter 5 - Quantize of scattering theory. In *Synthetic Aperture Radar Imaging Mechanism for Oil Spills*, Marghany, M., Ed. Gulf Professional Publishing: 2020; pp 73-92.

10. Quan, B.; Liang, X.; Ji, G.; Cheng, Y.; Liu, W.; Ma, J.; Zhang, Y.; Li, D.; Xu, G., Dielectric polarization in electromagnetic wave absorption: Review and perspective. *Journal of Alloys and Compounds* **2017,** *728*, 1065-1075.
11. Jaramillo, R.; Ravichandran, J., In praise and in search of highly-polarizable semiconductors: Technological promise and discovery strategies. *APL Materials* **2019,** *7* (10), 100902.
12. Vadlamudi, V. E., M.; Banerjee, P. K.; Raihan, R.; Reifsnider, K. In *Study of Defect Coalescence in Heterogeneous Material Systems using Broad Band Dielectric Spectroscopy*, American Society for Composites: Thirty-Second Technical Conference, Purdue University, West Lafayette, Indiana, October 23-25, 2017; DEStech Publications: Purdue University, West Lafayette, Indiana, 2017.
13. Chen, R. First-Principles Study on Electronic and Optical Properties of Copper-Based Chalcogenide Photovoltaic Materials. Doctoral Thesis, KTH Royal Institute of Technology, Stockholm, Sweden, 2017.
14. Kremer, F.; Schönhals, A., *Broadband Dielectric Spectroscopy*. 1 ed.; Springer, Berlin, Heidelberg: 2003.
15. Pozar, D. M., *Microwave engineering* 4th Edition ed.; J. Wiley: Hoboken, NJ, 2012.
16. Kwon, D.; Azarian, M. H.; Pecht, M., Early Detection of Interconnect Degradation by Continuous Monitoring of RF Impedance. *IEEE Transactions on Device and Materials Reliability* **2009,** *9* (2), 296-304.
17. Azarian, M. H.; Schneider, F. C. In *The role of impedance control in early detection of interconnect degradation using time domain reflectometry*, 2012 IEEE 16th Workshop on Signal and Power Integrity (SPI), 13-16 May 2012; 2012; pp 21-24.
18. Okoro, C.; Kabos, P.; Obrzut, J.; Hummler, K.; Obeng, Y. S. In *Use of RF- based technique as a metrology tool for TSV reliability analysis*, Electronic Components and Technology Conference (ECTC), 2013 IEEE 63rd, IEEE: 2013; pp 186-191.
19. Okoro, C.; Levine, L. E.; Xu, R.; Hummler, K.; Obeng, Y., Synchrotron-based measurement of the impact of thermal cycling on the evolution of stresses in Cu through- silicon vias. *Journal of Applied Physics* **2014,** *115* (24), 243509.
20. Obeng, Y. S.; Okoro, C. A.; Amoah, P. K.; Franklin, R. R.; Kabos, P., Low Frequency Radio Wave Detection of Electrically Active Defects in Dielectrics. *ECS Journal of Solid State Science and Technology* **2015,** *5* (4), P3025-P3030.
21. Beall Fowler, W.; Edwards, A. H., Theory of defects and defect processes in silicon dioxide. *Journal of Non-Crystalline Solids* **1997,** *222*, 33-41.
22. Okoro, C. A.; Obeng, Y. S., A case study on the impact of local material chemistry on the mechanical reliability of packaged integrated circuits: Correlation of the packaging fallout to the chemistry of passivation dielectrics. *Thin Solid Films* **2012,** *520* (15), 5060-5063.
23. Jonscher, A. K., Dielectric relaxation in solids. *Journal of Physics D: Applied Physics* **1999,** *32* (14), R57.
24. Obeng, Y. S.; Okoro, C. A.; Amoah, P. K.; Dai, J.; Vartanian, V. H., Towards Understanding Early Failures Behavior during Device Burn-In: Broadband RF Monitoring of Atomistic Changes in Materials. *ECS Journal of Solid State Science and Technology* **2016,** *5* (9), N61-N66.
25. Mania, P.; Verel, R.; Jenny, F.; Hammond, C.; Hermans, I., Thermal Restructuring of Silica-Grafted TiClx Species and Consequences for Epoxidation Catalysis. *Chemistry – A European Journal* **2013,** *19* (30), 9849-9858.
26. Sunday, C. E.; Montgomery, K. R.; Amoah, P. K.; Iwuoha, E. I.; Obeng, Y. S., Broadband Dielectric Spectroscopic Characterization of Thermal Stability of Low-k Dielectric Thin Films for Micro- and Nanoelectronic Applications. In *Semiconductors,*

Dielectrics, and Metals for Nanoelectronics 15: In Memory of Samares Kar, Misra, D.; DeGendt, S.; Houssa, M.; Kita, K.; Landheer, D., Eds. 2017; Vol. 80, pp 253-264.

27. Obrzut, J., Surface conductance and microwave scattering in semicontinuous gold films. *ACTA IMEKO* **2015,** *4* (3), 42-46.
28. Su, K.; Bujalski, D. R.; Eguchi, K.; Gordon, G. V.; Ou, D.-L.; Chevalier, P.; Hu, S.; Boisvert, R. P., Low-k Interlayer Dielectric Materials: Synthesis and Properties of Alkoxy-Functional Silsesquioxanes. *Chemistry of Materials* **2005,** *17* (10), 2520-2529. 29. Lin, Y.; Jung-Joon, A.; Yaw, S. O.; Joseph, J. K., Subsurface imaging of metal lines embedded in a dielectric with a scanning microwave microscope. *Journal of Physics D: Applied Physics* **2016,** *49* (4), 045502.
30. Li, H.; Zhu, H.; Yuan, H.; You, L.; Richter, C. A.; Kopanski, J. J.; Zhao, E.; Li, Q., SnTe field effect transistors and the anomalous electrical response of structural phase transition. *Applied Physics Letters* **2014,** *105* (1), 013503.
31. Yuan, H.; Cheng, G.; You, L.; Li, H.; Zhu, H.; Li, W.; Kopanski, J. J.; Obeng, Y. S.; Hight Walker, A. R.; Gundlach, D. J.; Richter, C. A.; Ioannou, D. E.; Li, Q., Influence of Metal–MoS2 Interface on MoS2 Transistor Performance: Comparison of Ag and Ti Contacts. *ACS Applied Materials & Interfaces* **2015,** *7* (2), 1180-1187. 32.

Imtiaz, A.; Wallis, T. M.; Kabos, P., Near-Field Scanning Microwave Microscopy: An Emerging Research Tool for Nanoscale Metrology. *IEEE Microwave Magazine* **2014,** *15* (1), 52-64.